ACS OMEGA

http://pubs.acs.org/journal/acsodf

Article

# Degradable Carrageenan as a Substrate and Resistive Material for Flexible Applications

Yu-Chi Chang* and Chih-Hsin Lin

Cite This: *ACS Omega* 2023, 8, 12387−12392

Read Online

ACCESS | Metrics & More | Article Recommendations

**ABSTRACT:** In recent years, due to the environmental impact caused by electronic waste, decomposable components have become one of the most important topics in the world. In this study, the carrageenan material extracted from red algae was used as the resistance-switching layer of electronic components, and potassium was added to the carrageenan as a substrate (CK). CK has the advantages of excellent mechanical properties, transparency, and decomposability. In addition, the In/carrageenan/Ag/CK (ICACK) device exhibits good memory properties with a high ON/OFF ratio exceeding $10^7$ and a retention time exceeding $10^4$ s. Due to the doping of potassium ions, the ICACK element has a fairly good bending performance. Although bending or stretching under a small radius of curvature will not have a great impact on the electrical performance, it shows that in the future wearable or good potential in the field of implantable devices.

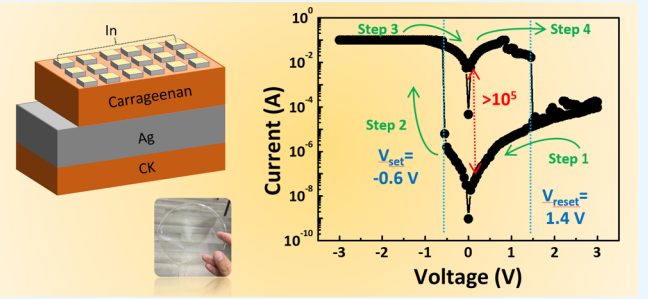


## 1. INTRODUCTION

Resistance random access memory (RRAM) has attracted a great deal of attention in recent years due to its nonvolatility, high-speed performance, high-density, fast response time, low power consumption, and simple structure.[1] Owing to the advantages of structural flexibility and low-temperature solution process-ability biomaterials, resistive layers have been recognized as an emerging candidate for next-generation nonvolatile memory applications.[2,3] On the other hand, because more and more wearable and biointegrated medical devices are being developed to improve the convenience and security of our lives,[4] biodegradable flexible memory devices are rapidly rising all over the world.[5,6] The stability of each layer comprising the flexible resistive memory device determines the performance of a biodegradable flexible memory device under structurally bent conditions. Furthermore, their bending performance also depends on the mechanical properties of biodegradable substrates. Thus, a key step toward achieving a biodegradable flexible memory device is to seek suitable biodegradable substrates. An ideal biodegradable substrate should not only be eco-friendly but also flexible, such as the capability to prevent the structural fractures of electrode materials or provide an acceptable performance level for memory applications under structurally bent conditions.

The carrageenan material is a polysaccharide extracted from seaweed, which is used in the pharmaceutical, medical, cosmetic, and food fields. It has many advantages, including low cost and abundance in nature.[7,8] In recent years, carrageenan has attracted considerable attention because of its biodegradability, biocompatibility, low cost, abundance in nature, and nontoxicity.[9] In addition, since carrageenan is a highly flexible molecule that forms a coiled helical structure, is recycled, and has the excellent film-forming capacity, it is ideal for the fabrication of flexible biosubstrate.

In 2016, Liu and Li's group reported that the mechanical properties and recoverability of carrageenan hydrogel could be improved using a physical cross-linker (KCl).[10] It was found that the elastic modulus ($E$) of the hydrogel increased with increasing $K^+$ contents.

In this work, the flexible biosubstrate has been successfully fabricated by using carrageenan mixed with $KNO_3$ salts (CK). Additionally, the carrageenan material was used as a resistive layer to develop a strong adhesive interface between the substrate and the bottom electrode/resistive layer. A strong adhesive interface can enhance the bending performances of flexible electronic devices.[11] As a flexible, biodegradable device, its degradability, stability, and mechanical properties should receive special attention. Therefore, the resistive switching characteristics and mechanical flexibility of a In/carrageenan/Ag sandwich structure on a biosubstrate (ICACK) were investigated. Its mechanical flexibility is also investigated as a

Received: January 10, 2023
Accepted: March 15, 2023
Published: March 27, 2023

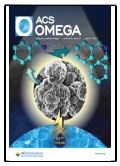

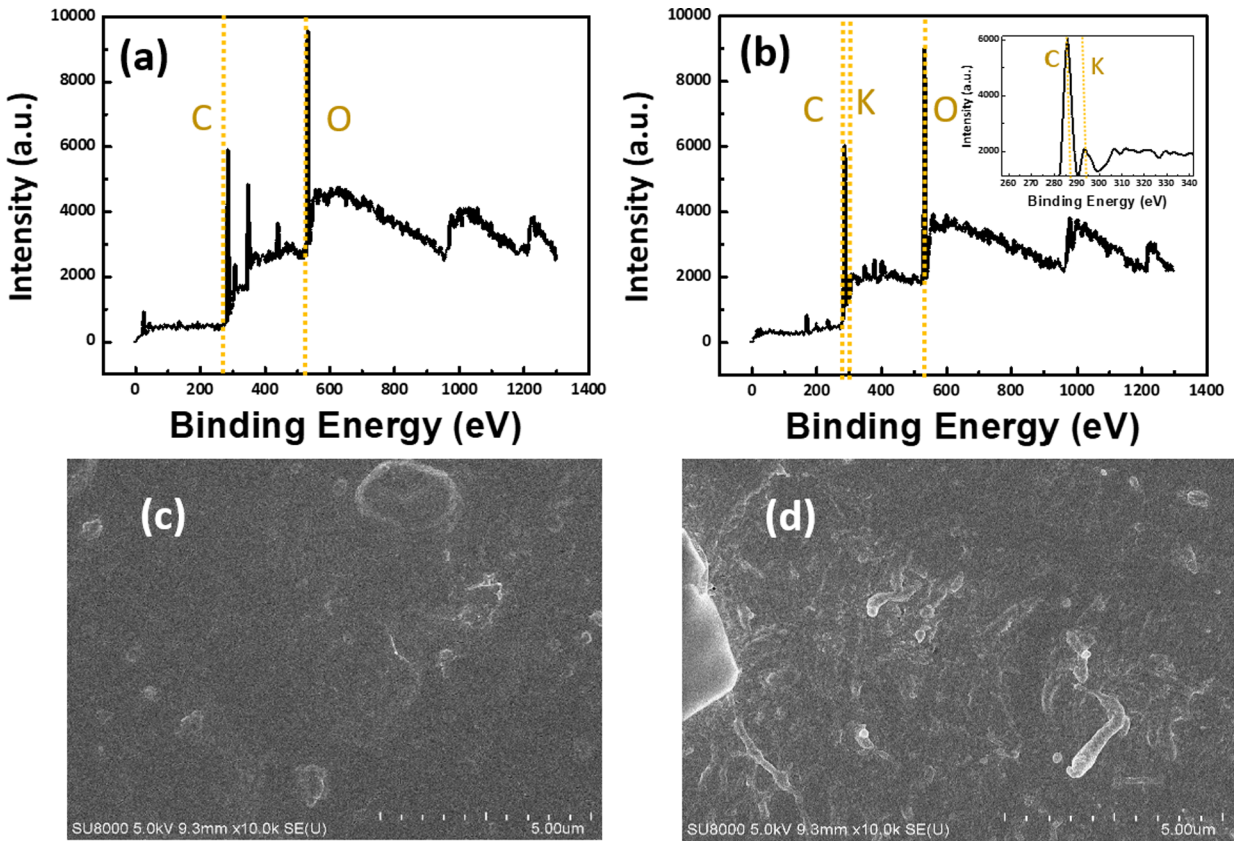


**Figure 1.** XPS analyses of (a) CP and (b) CK. SEM image of (c) CP and (d) CK.

function of the bending radius and the number of repeated bending tests to exhibit its potential for eco-friendly flexible memory devices. The decomposition time of the whole device was 52 days. In the near future, this eco-friendly flexible memory device can be useful for wearable electronics for medical physiology assessment.

## 2. DEVICE STRUCTURE AND FABRICATION

**2.1. Substrate Preparation.** To fabricate a smooth, uniform, excellent mechanical properties, and biodegradable carrageenan substrate, we prepare carrageenan solution with a concentration of 2% by mixing carrageenan powder 1.6327 g, $KNO_3$ powder 0.1306 g, and 80 mL deionized water in a beaker with a magnetic stirrer for 3 h. In addition, to unravel the double helix structure in carrageenan, we raised the temperature to 90 °C to make sure it thoroughly dissolved, and at last, let it stand under 90 °C for 1 h to diminish bubbles. After the solution is ready, we cast it into a plastic petri dish with a diameter of 17 cm and put it in the refrigerator cooling for a day, ensuring the double helix formation to improve the mechanical strength. Afterward, dried it in a cycling oven at 40 °C for 30 h to evaporate the remaining solvent (water).

**2.2. Device Preparation.** First, we cut down a piece of appropriate size of carrageenan substrate, then fabricated the silver bottom electrode. The conductive silver paint is obtained from SPI Supplies, and at first, we diluted it with alcohol, then the sliver paste was painted onto the prepared carrageenan substrate and dried in a cycling oven at 50 °C for 30 min to remove the redundant solvent. After that, we made a thin film as a resistive layer, the carrageenan solution was prepared from carrageenan powder (supplied by Sigma) and dissolved in deionized water with a magnetic stirrer for 1 h with heating at 90 °C to ensure that the carrageenan solution thoroughly dissolved. Then, the carrageenan solution was spin-coated at room temperature onto the silver bottom electrode layer as a resistive layer. After the deposition of carrageenan thin film by spin coating, the device was baked in a cycling oven at 50 °C for 30 min to ensure the resistive layer formed evenly. The last step, flatten and cut the indium ball into several pieces then hot melt the indium ball by welding to make it adhere to the carrageenan dielectric layer to complete the top electrode. Finally, the fabrication of the In/carrageenan/Ag/carrageenan substrate is complete.

**2.3. Instrumentation.** The electrical properties were characterized by a Keithley 2636B system source meter. Scanning electron microscope (SEM, Hitachi SU8000) analysis was employed to observe the cross-sectional and top-view of samples. The transmittance of the sample was confirmed by ultraviolet and visible absorption spectroscopy (UV−vis) with Perkin-Elmer Lambda 35. Atomic force microscope (AFM) analysis (Dimension ICON with Nano-Scope V controller, Bruker, USA) was used to characterize the surface morphology. X-ray photoelectron spectroscopy (XPS) was carried out using the PHI 5000 Versa Probe. Nano-indenter analysis was conducted by Nano-Indentation System I, MTS XP.

## 3. RESULTS AND DISCUSSION

To determine the total elemental composition of CP and CK, XPS analyses were conducted. As shown in Figure 1a,b, the composition of CP was 64.8% of C and 35.2% of O, and the composition of CK is 59.7% of C, 35.4% of O, and 4.9% of


https://doi.org/10.1021/acsomega.3c00165
ACS Omega 2023, 8, 12387−12392

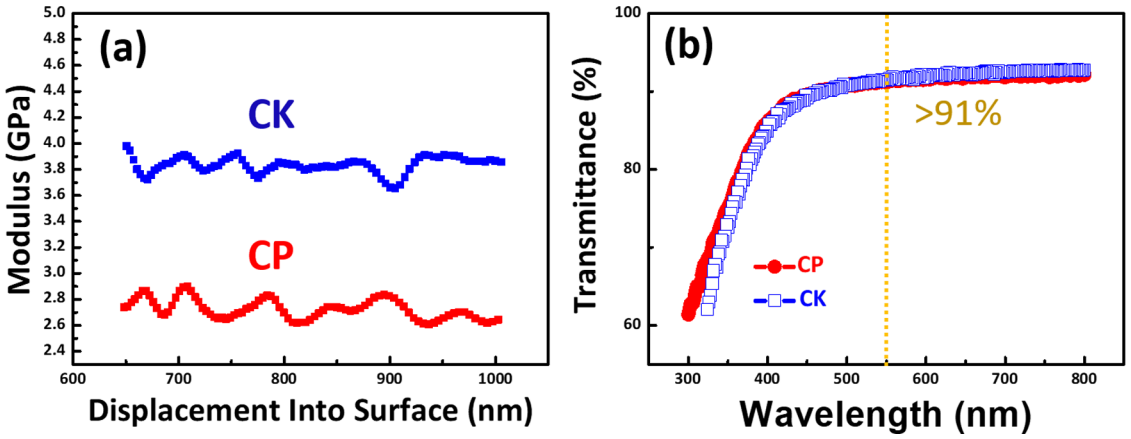


**Figure 2.** (a) Modulus of the CP and CK. The inset shows the photograph of the synthesized transparent of CK and (b) the UV−vis transmittance spectra.

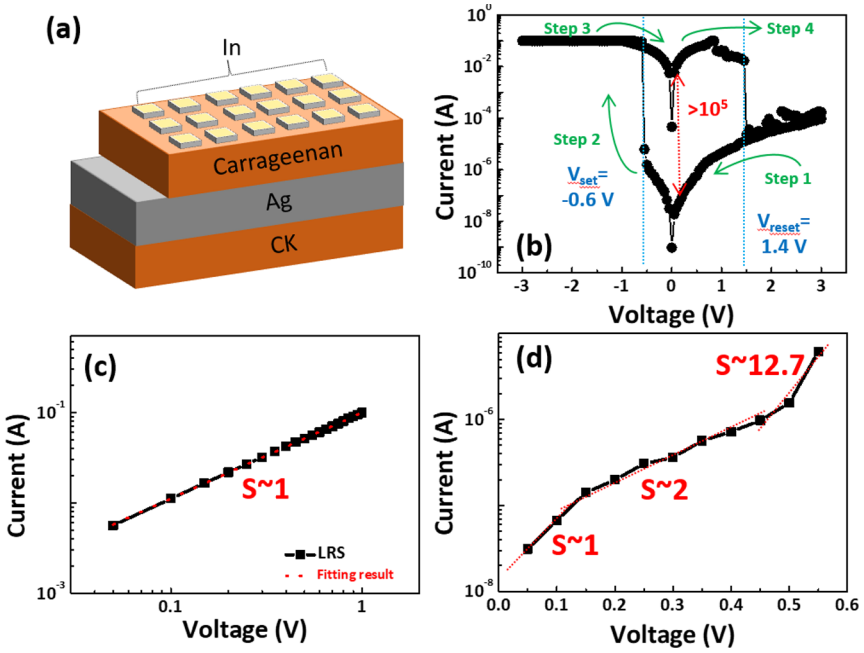


**Figure 3.** (a) Structure of the ICACK device. (b) *I*−*V* switching characteristic of the ICACK device. Linear fitting and corresponding slopes of ICACK for (c) LRS and (d) HRS.

K.[12−14] To investigate the effect of adding potassium ions on the microstructure of carrageenan, Figure 1c,d shows the SEM micrographs of pure carrageenan substrate (CP) and CK, respectively. It can be observed that after adding potassium ions, several coil-to-double helix structures appeared which proves that potassium ions will indeed affect the structure of CS.[15] In addition, the aggregation of molecules enhances the mechanical properties of CS, which make it has better bending ability and can be applied in a broader field.

Figure 2a shows the modulus of CP and CK obtained from nanoindenter analysis, and the modulus of CP and CK was 2.7 and 3.8 GPa, respectively.[16] The relatively larger modulus of CK can be attributed to the coil-to-double helix structures. This result makes the device have better bending ability, allowing the device to perform better under uneven or external force conditions.

The addition of potassium nitrate does not have any impact on the transparency. Figure 2b shows the UV−vis spectrum of CP and CK. The transmittance of CS and CK at 550 nm is higher than 91%. It is indicated the doping of potassium ion changes the microstructure but does not affect light transmission. This excellent property also makes CK great potential and is competitive for optoelectronic devices.

In order to further understand the characteristics of CK substrate applied to RRAM, the flexible In/carrageenan/Ag/CK (ICACK) structure was fabricated and electrical measurements were performed. Figure 3a shows the device structure of the ICACK device. The *I*−*V* characteristic of the ICACK device exhibited bipolar resistive switching behavior, as shown in Figure 3b. When applying negative bias, the conductive filament formed, switching the current state from HRS to LRS without the forming operation. With applying positive bias, the filament was ruptured, and the reset occurred, switching the current state back to HRS. The ON/OFF ratio was calculated by the current value under 0.1 V of LRS and HRS, and the average magnitude can be up to 7 orders, showing the good data storage ability of this device.



https://doi.org/10.1021/acsomega.3c00165
ACS Omega 2023, 8, 12387−12392

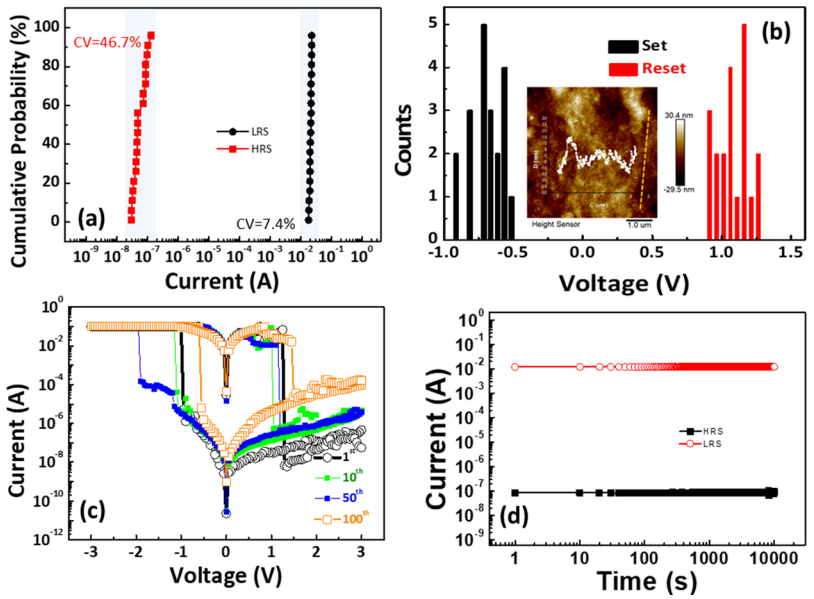


**Figure 4.** (a) Statistic distribution of the HRS and LRS current values for the ICACK device under a read bias of 0.1 V. (b) Statistic distribution of the set and reset voltage values for the ICACK device. The inset shows 2D AFM topography of CK. (c) Bending property of ICACK device. (d) Retention time of LRS and HRS current under read bias 0.1 V.

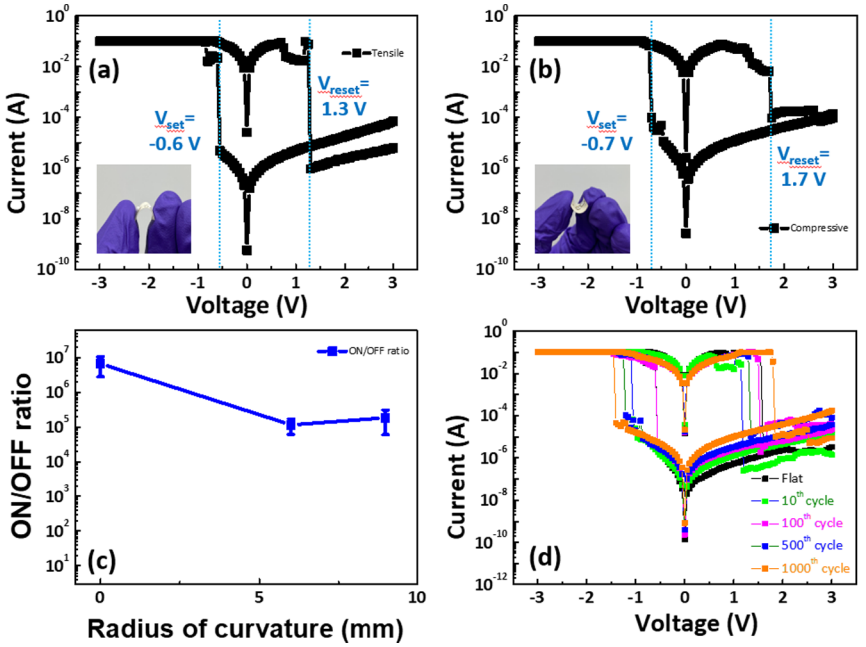


**Figure 5.** *I*−*V* curve of ICACK device under (a) tensile and (b) compressive conditions with a radius of curvature of 6 mm. (c) ON/OFF ratio as a function of different radii of curvature for the ICACK device under the compressive condition. (d) *I*−*V* curve of the ICACK device according to bending cycles.

To further investigate the conduction mechanism of the ICACK device, the LRS and HRS current of the *I*−*V* curve was re-plotted into a log−log scale as shown in Figure 3c,d. The slope of the LRS current approaches to 1 after fitting, and this result corresponds well with the ohmic conduction mechanism.[17] The HRS current can be divided into three different segments, and the slopes of each segment are approximately 1, 2, and 12.7, respectively. The slope of the first segment indicates that conduction follows the ohmic conduction mechanism, the second segment corresponds to the child's law ($I \propto V^2$), and the current at the third segment increases steeply, indicating the formation of filament ($I \propto V^n$). The above results suggest that the mechanism of HRS follows the space-charge limited conduction (SCLC).[18]

Figure 4a,b shows the uniformity of the ICACK device. The currents of the LRS and HRS were measured at 0.1 V. The coefficient of variation (CV) can be used to define the uniformity of a device. The CVs of $I_{HRS}$ and $I_{LRS}$ are 46.7 and 7.4%, respectively. Figure 4b shows the distribution of $V_{set}$ and $V_{reset}$. The average value of $V_{set}$ is −0.7 V and in the range of −0.5 to −0.9 V. The average of $V_{reset}$ is 1 V and in the range of 0.9−1.25 V. Figure 4c shows the switching cycles of the ICACK device, the ON/OFF ratio could be maintained over $10^5$ after switching 100 cycles. Figure 4d shows the retention


https://doi.org/10.1021/acsomega.3c00165
ACS Omega 2023, 8, 12387−12392

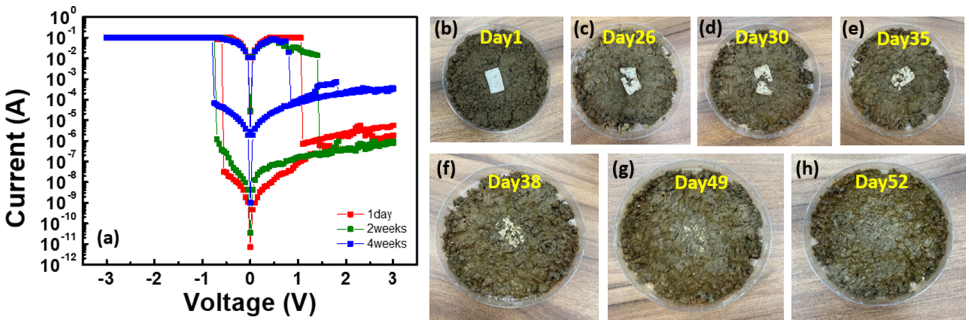


**Figure 6.** (a) Aging time for the ICACK device. (b–h) Degradability of the ICACK device.

time was over $10^4$ s. The excellent uniformity and stability can be attributed to the rough substrate due to the strong electric field generated at the tip, there is high repeatability in forming the filament, and at the same time, a lower set voltage is required.

The 2D AFM image shows that the root mean square roughness was around 8.4 nm. Owing to the rougher surface of the substrate, the bottom electrode will have more tip-like topography, which will enhance the local electric field,[19] making the filament easier to form and the set voltage may be lower.

As a wearable application, the durability of a biosubstrate is one of the most important properties, so the flexibility of the ICACK device was measured. Figure 5a,b shows the resistive switching characteristics of the ICACK device at a radius of curvature of 6 mm in tension and compression, respectively. The bipolar resistive switching behavior of devices is well preserved under two different bending conditions. The set/reset voltages of the device under tensile and compressive conditions are −0.6/1.3 and −0.7/1.7, respectively. Whether the devices are tensile or compressive, their set/reset voltage values are similar to those in the flat state. However, a lower ON/OFF ratio of the device under stressed conditions was observed compared to the device in the flat state. The ON/OFF ratio of the device under tensile and compressive conditions are around $6 \times 10^4$ and $10^4$, respectively. Significant attenuation of these ON/OFF ratios is associated with reduced adhesion between the In electrode and the carrageenan layer.

Figure 5c shows the ON/OFF ratio as a function of different radii of curvature for the device measured directly under compressive bending conditions. When the bending radius is reduced to 6 mm, the ON/OFF ratio can maintain above $10^4$, proving that the ICACK device can be applied to various conditions. Figure 5d shows the bending property of the ICACK device. Although the ON/OFF ratio decreased slightly after 1000 cycles, the ON/OFF ratio can still maintain a magnitude over $10^4$ with excellent bipolar RS behavior.

Figure 6a shows the aging time for the ICACK device. The device was measured and stored under ambient conditions (at room temperature: ∼26 °C, relative humidity: ∼60%) for 30 days. In the first 2 weeks, the electrical performance was still great, and the ON/OFF ratio did not decrease significantly. However, after 30 days, the ON/OFF ratio dropped and became relatively unstable. It is speculated that this may be due to the ambient humidity affecting the resistive layer and the electrodes, causing the hydrogel itself to absorb water and the electrodes to oxidize,[20,21] and these can be surmounted in future packaging. Figure 6b–h shows the degradability of the ICACK device. The ICACK device degrades completely within 52 days. The rapid degradation of the ICACK device demonstrates the potential for application in green electronics and medical implantable devices, enabling the development of the field of electronic devices in a sustainable and environmental-friendly direction.

## 4. CONCLUSIONS

In summary, a fully biodegradable ICACK device with a high ON/OFF ratio $>10^7$ and excellent flexibility can be investigated by a low-cost and simple solution-based process. The mechanical properties of the carrageenan substrate were improved by adding potassium ions, and the modulus was increased from 2.7 to 3.8 GPa. The device uses carrageenan as both the resistive layer and the substrate material, so the device has excellent uniformity, flexibility, and stability, for example, under a 6 mm radius of curvature and 1000 bending cycles, the device still maintains a good bipolar RS behavior with a magnitude of the ON/OFF ratio greater than $10^4$; the CV of the HRS current is 46.7%; the retention time can be reached more than $10^4$ s; the required set voltage is lower than 1 V. In addition, the addition of potassium nitrate does not have any impact on the transparency or biodegradability. As the above results, ICACK devices have fabulous development potential in bioelectronic devices in the future.

## AUTHOR INFORMATION

### Corresponding Author

**Yu-Chi Chang** − *Department of Engineering Science, National Cheng Kung University, Tainan 70101, Taiwan;*
orcid.org/0000-0003-2253-935X;
Email: christina780712@gmail.com

### Author

**Chih-Hsin Lin** − *Department of Engineering Science, National Cheng Kung University, Tainan 70101, Taiwan*

Complete contact information is available at:
https://pubs.acs.org/10.1021/acsomega.3c00165

### Notes

The authors declare no competing financial interest.

## ACKNOWLEDGMENTS

This research is sponsored by the National Science and Technology Council of Taiwan under Grant no. MOST 111-2636-E-006-029.

## ABBREVIATIONS

| | |
|---|---|
| CK | carrageenan substrate with $KNO_3$ salt |
| ICACK | In/carrageenan/Ag/CK |



https://doi.org/10.1021/acsomega.3c00165
ACS Omega 2023, 8, 12387−12392

T.E. top electrode
B.E. bottom electrode

## REFERENCES


(1) Shen, Z.; Zhao, C.; Qi, Y.; Xu, W.; Liu, Y.; Mitrovic, I. Z.; Yang, L.; Zhao, C. Advances of RRAM devices: Resistive switching mechanisms, materials and bionic synaptic application. *Nanomaterials* **2020**, *10*, 1437.

(2) Rehman, M. M.; Ur Rehman, H. M. M.; Kim, W. Y.; Sherazi, S. S. H.; Rao, M. W.; Khan, M.; Muhammad, Z. Biomaterial-based nonvolatile resistive memory devices toward ecofriendliness and biocompatibility. *ACS Appl. Electron. Mater.* **2021**, *3*, 2832−2861.

(3) Park, I.; Cheng, J.; Pisano, A. P.; Lee, E. S.; Jeong, J. H. Low temperature, low pressure nanoimprinting of chitosan as a biomaterial for bionanotechnology applications. *Appl. Phys. Lett.* **2007**, *90*, No. 093902.

(4) Ray, T. R.; Choi, J.; Bandodkar, A. J.; Krishnan, S.; Gutruf, P.; Tian, L.; Ghaffari, R.; Rogers, J. A. Bio-integrated wearable systems: a comprehensive review. *Chem. Rev.* **2019**, *119*, 5461−5533.

(5) Liu, S.; Dong, S.; Wang, X.; Shi, L.; Xu, H.; Huang, S.; Luo, J. Flexible and fully biodegradable resistance random access memory based on a gelatin dielectric. *Nanotechnology* **2020**, *31*, 255204.

(6) Huang, W. Y.; Chang, Y. C.; Sie, Y. F.; Yu, C. R.; Wu, C. Y.; Hsu, Y. L. Bio-Cellulose Substrate for Fabricating Fully Biodegradable Resistive Random Access Devices. *ACS Appl. Polym. Mater.* **2021**, *3*, 4478−4484.

(7) Li, L.; Ni, R.; Shao, Y.; Mao, S. Carrageenan and its applications in drug delivery. *Carbohydr. Polym.* **2014**, *103*, 1−11.

(8) Pacheco-Quito, E. M.; Ruiz-Caro, R.; Veiga, M. D. Carrageenan: drug delivery systems and other biomedical applications. *Mar. Drugs* **2020**, *18*, 583.

(9) de Lima Barizão, C.; Crepaldi, M. I.; Oscar de Oliveira, S.; de Oliveira, A. C.; Martins, A. F.; Garcia, P. S.; Bonafé, E. G. Biodegradable films based on commercial κ-carrageenan and cassava starch to achieve low production costs. *Int. J. Biol. Macromol.* **2020**, *165*, 582−590.

(10) Liu, S.; Li, L. Recoverable and self-healing double network hydrogel based on κ-carrageenan. *ACS Appl. Mater. Interfaces* **2016**, *8*, 29749−29758.

(11) Chang, Y. C.; Liu, H. J.; Lin, K. W.; Huang, W. Y.; Hsu, Y. L. A Biodegradable Gelatin Substrate and its Application for Crack Suppression of Flexible Gelatin Resistive Memory Device. *Adv. Electron. Mater.* **2022**, No. 2101014.

(12) Lima, P. H.; Pereira, S. V.; Rabello, R. B.; Rodriguez-Castellón, E.; Beppu, M. M.; Chevallier, P.; Mantovani, D.; Vieira, R. S. Blood protein adsorption on sulfonated chitosan and κ-carrageenan films. *Colloids Surf., B* **2013**, *111*, 719−725.

(13) Berton, S. B.; de Jesus, G. A.; Sabino, R. M.; Monteiro, J. P.; Venter, S. A.; Bruschi, M. L.; Popat, K. C.; Matsushita, M.; Martin, A. F.; Bonafé, E. G. Properties of a commercial κ-carrageenan food ingredient and its durable superabsorbent hydrogels. *Carbohydr. Res.* **2020**, *487*, No. 107883.

(14) Li, Z.; Wang, F.; Liu, C.; Gao, F.; Shen, L.; Guo, W. Efficient perovskite solar cells enabled by ion-modulated grain boundary passivation with a fill factor exceeding 84%. *J. Mater. Chem. A* **2019**, *7*, 22359−22365.

(15) Mangione, M. R.; Giacomazza, D.; Bulone, D.; Martorana, V.; San Biagio, P. L. Thermoreversible gelation of κ-Carrageenan: relation between conformational transition and aggregation. *Biophys. Chem.* **2003**, *104*, 95−105.

(16) Liu, S.; Li, L. Ultrastretchable and self-healing double-network hydrogel for 3D printing and strain sensor. *ACS Appl. Mater. Interfaces* **2017**, *9*, 26429−26437.

(17) Lee, J. H.; Park, S. P.; Park, K.; Kim, H. J. Flexible and waterproof resistive random-access memory based on nitrocellulose for skin-attachable wearable devices. *Adv. Funct. Mater.* **2020**, *30*, No. 1907437.

(18) Cheong, K. Y.; Tayeb, I. A.; Zhao, F.; Abdullah, J. M. Review on resistive switching mechanisms of bio-organic thin film for non-volatile memory application. *Nanotechnol. Rev.* **2021**, *10*, 680−709.

(19) Zhang, W.; Tang, J.; Gao, B.; Sun, W.; Liu, W.; Wang, K.; Wu, W.; Qian, H.; Wu, H. Impact of Bottom Electrode Roughness on the Analog Switching Characteristics in Nanoscale RRAM Array. In *2021 Device Research Conference (DRC)*; IEEE, 2021; pp 1−2.

(20) Dankoco, M. D.; Tesfay, G. Y.; Benevent, E.; Bendahan, M. Temperature sensor realized by inkjet printing process on flexible substrate. *Mater. Sci. Eng., B* **2016**, *205*, 1−5.

(21) Chang, Y. C.; Wang, Y. H. Resistive switching behavior in gelatin thin films for nonvolatile memory application. *ACS Appl. Mater. Interfaces* **2014**, *6*, 5413−5421.




https://doi.org/10.1021/acsomega.3c00165
*ACS Omega* 2023, 8, 12387−12392